Optical variability modelling of newly identified blazars and blazar candidates behind Magellanic Clouds

[1,2]Natalia Żywucka-Hejzner
In collaboration with
[2]Mariusz Tarnopolski, [2]Volodymyr Marchenko, [2]Łukasz Stawarz, [1]Markus Boettcher, [3]Szymon Kozłowski, and [3]Andrzej Udalski

[1]Nort-West University, [2]Astronomical Observatory of Jagiellonian University, and [3]Warsaw University

HEPRO VII, July 2019

Credit: imgur.com/JADDgSL

The work was supported by the Polish National Science Center (NCN) through the PRELUDIUM grant DEC-2014/15/N/ST9/05171.

Table of Contents

Credit: ESO/S.Brunier

The Optical Gravitational Lensing Experiment
OGLE

OGLE project: since 1992;
Andrzej Udalski

Main scientific goals:

- MCs and Galactic Bulge monitoring,
- dark matter study with microlensing phenomena,
- extrasolar planets' searching,
- galactic structure study,
- analysis of different time scale variability of hundred millions regularly observed objects.

Location: Las Campanas, Chile.

Credit: Prof. I. Soszyński

Magellanic Quasars Survey
MQS

- Sky coverage of the MQS: 100% of the LMC and 70% of the SMC
- Targets from OGLE-III
- Selection based on mid-IR and optical colours, optical variability, X-ray properties, and optical spectroscopy
- Confirmation of 758 quasars (565 in the LMC and 193 in the SMC)
- 94% quasars from the MQS catalogue (527 in the LMC and 186 in the SMC) are newly identified objects

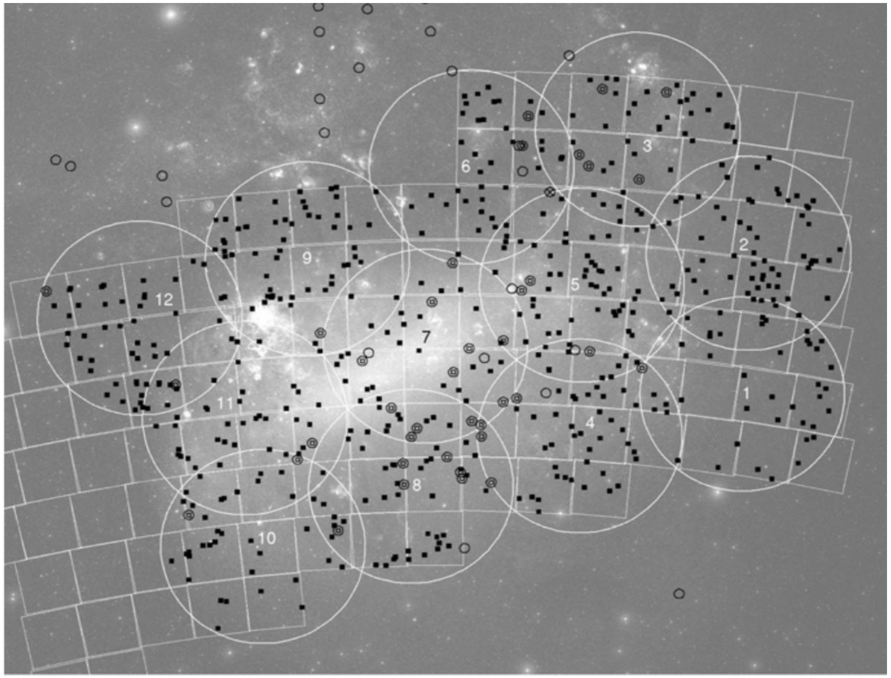

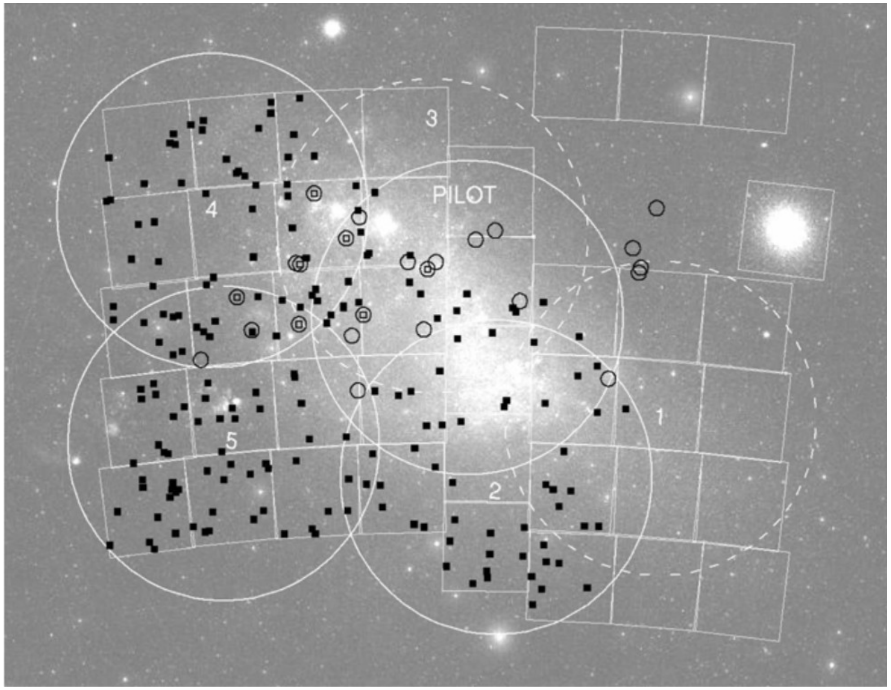

Credit: Kozłowski et al. 2013

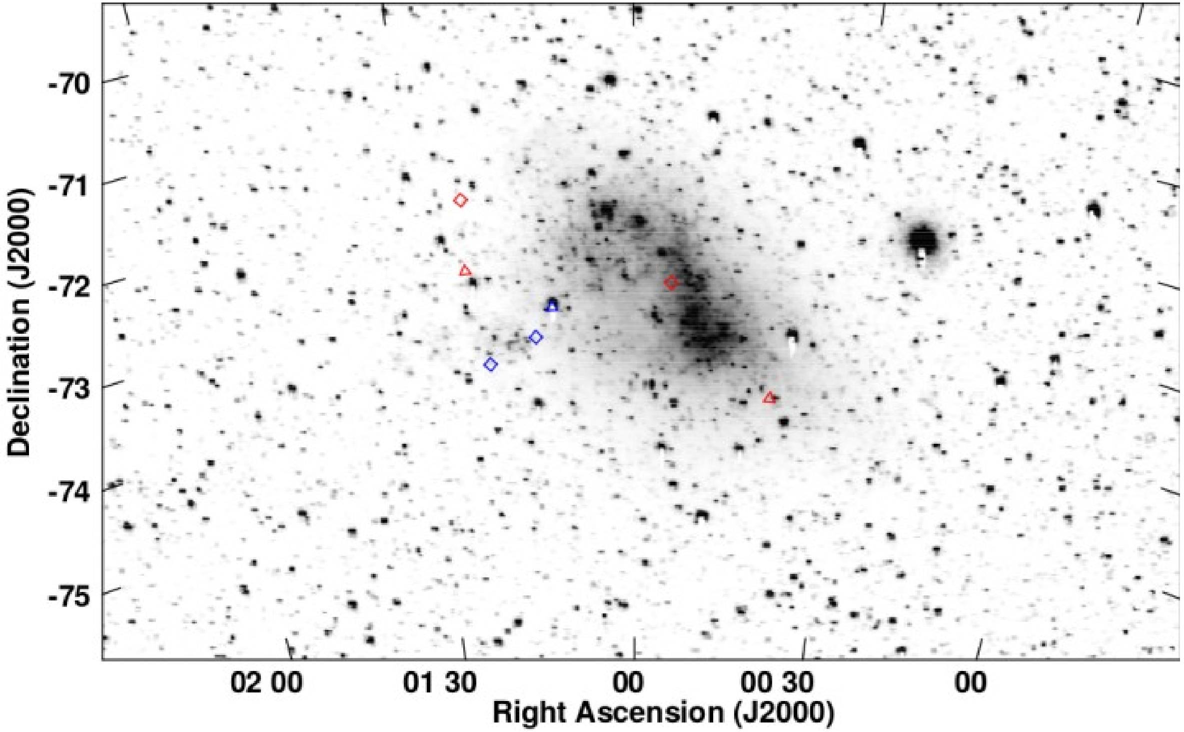

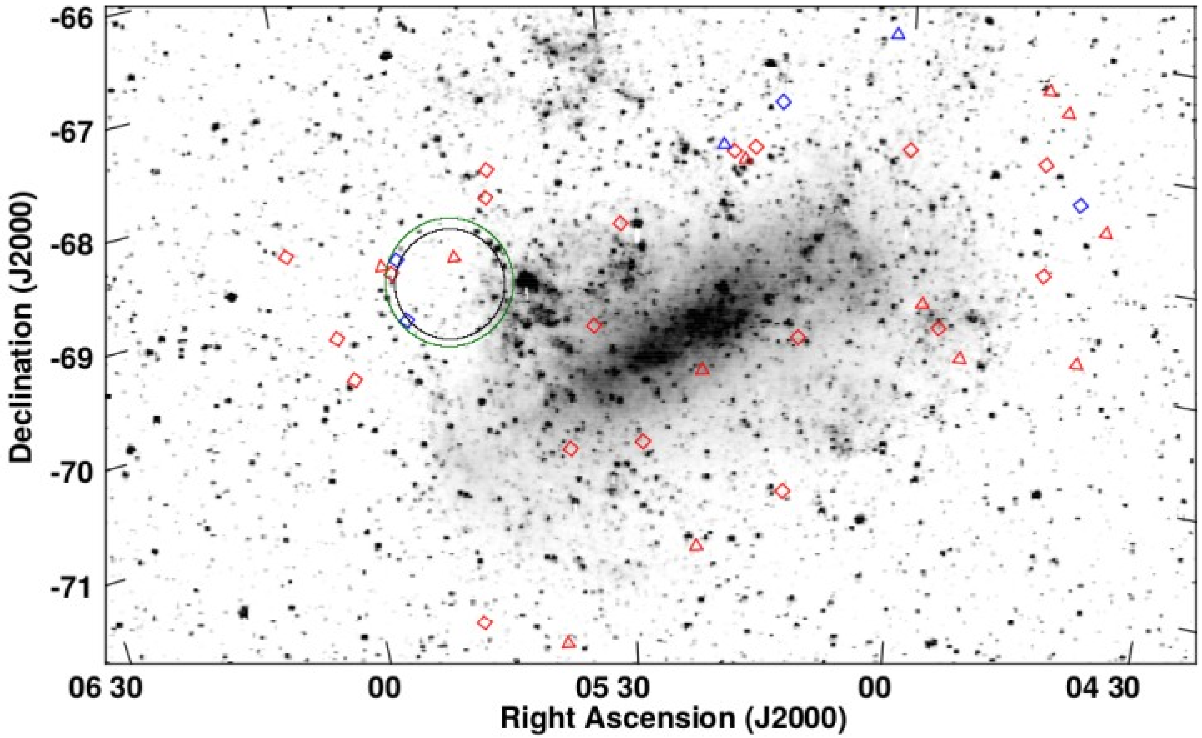

Optical image: Bothun & Thompson (1988)

- 44 sources selected:
  27 FSRQs
  17 BL Lacs
- faint sources with 16 – 21 mag_I
- distant sources with z = 0.3 – 3.3
- radio-loudness:
  FSRQs: 12 – 4 450
  BL Lacs: 171 – 7 020
- radio spectral index:
  from -0.57 up to 1.37
- IR spectral index:
  from -0.44 up to 3.07
- average polarization of $PD_{r,4.8}$ ~ 6.8% at 4.8 GHz
- possible association with flarying source detected by Fermi-LAT

Optical variability study of all blazar candidates

- Motivation

→ to look for blazar-like characteristics
→ to analyse the long-term behaviour
→ to search for the quasi-periodic oscillations.

- Data

Optical variability study in filters I and V of both blazar candidates based on OGLE-II (1996-2000), OGLE-III (2001-2009), and -IV (2010-now) data
→ temporal coverage of > 20 years.

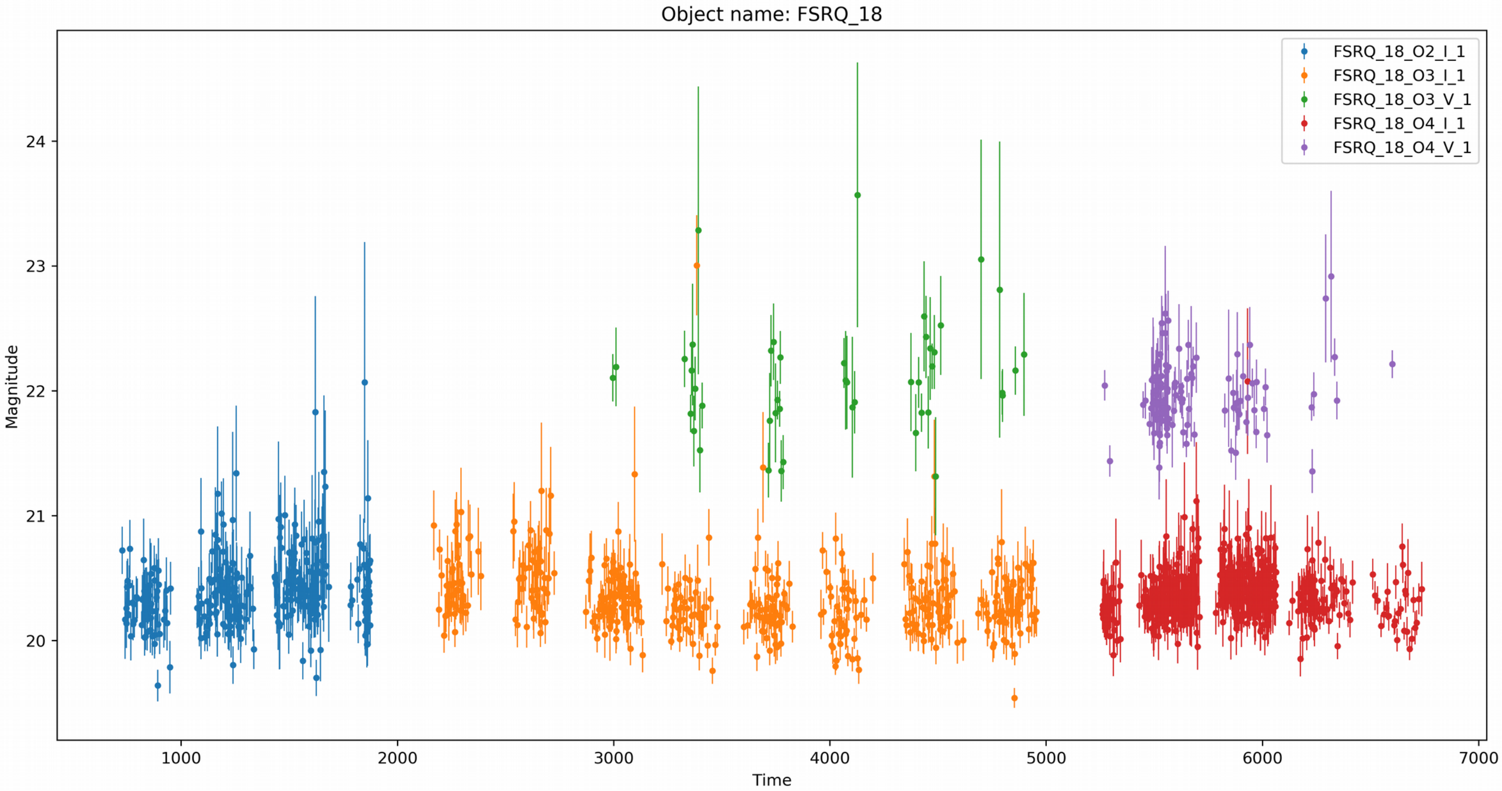

Optical variability study of all blazar candidates
methodology

- Lomb-Scargle periodograms
  power spectral density (PSD) for unevenly sampled time series:

$$P_{LS}(\omega) = \frac{1}{2\sigma^2}\left[\frac{\left(\sum_{k=1}^{N}(x_k-\bar{x})\cos[\omega(t_k-\tau)]\right)^2}{\sum_{k=1}^{N}\cos^2[\omega(t_k-\tau)]} + \frac{\left(\sum_{k=1}^{N}(x_k-\bar{x})\sin[\omega(t_k-\tau)]\right)^2}{\sum_{k=1}^{N}\sin^2[\omega(t_k-\tau)]}\right]$$

PL + Poisson noise: $P(f) = \frac{P_{\rm norm}}{f^{\beta}} + C$

smoothly broken PL (SBPL) plus Poisson noise:

$$P(f) = \frac{P_{\rm norm} f^{-\beta_1}}{1+\left(\frac{f}{f_{\rm break}}\right)^{\beta_2-\beta_1}} + C$$

- zero-mean Continuous-time Auto-Regressive Moving Average (CARMA) modelling

differential equation of stochastic processes:

$$\frac{{\rm d}^p x(t)}{{\rm d}t^p} + \alpha_{p-1}\frac{{\rm d}^{p-1}x(t)}{{\rm d}t^{p-1}} + \ldots + \alpha_0 x(t) = \beta_q\frac{{\rm d}^q\varepsilon(t)}{{\rm d}t^q} + \beta_{q-1}\frac{{\rm d}^{q-1}\varepsilon(t)}{{\rm d}t^{q-1}} + \ldots + \varepsilon(t)$$

PSD:

$$P_{\rm CARMA}(f) = \sigma^2\frac{\left|\sum_{j=0}^{q}\beta_j(2\pi {\rm i} f)^j\right|^2}{\left|\sum_{k=0}^{p}\alpha_k(2\pi {\rm i} f)^k\right|^2}$$

Ornstein-Uhlenbeck process for CARMA(1,0)
Lorentzian with a break frequency at $\alpha_0/(2\pi)$

$$P_{\rm OU}(f) = \frac{\sigma^2}{\alpha_0^2 + (2\pi f)^2}$$

Optical variability study of all blazar candidates
methodology

- Hurst exponent
  measures the statistical self similarity of a time series x(t): $x(t) \doteq \lambda^{-H} x(\lambda t)$

  autocorrelation function: $\rho(k) = \frac{1}{2}\left[(k+1)^{2H} - 2k^{2H} + (k-1)^{2H}\right]$

  Properties of Hurst exponent:

→ 0 < H < 1,
→ H = 1/2 for an uncorrelated process (e.g. white noise or Brownian motion),
→ H > 1/2 for a persistent (long-term memory, correlated) process,
→ H < 1/2 for an anti-persistent (short-term memory, anti-correlated) process.

- A-T Plane
  Abbe value, which quantifies the smoothness of a time serie

$$\mathcal{A} = \frac{\frac{1}{N-1}\sum_{i=1}^{N-1}(x_{i+1} - x_i)^2}{\frac{2}{N}\sum_{i=1}^{N}(x_i - \bar{x})^2}$$

  frequency relative to number of observations: $\mathcal{T} = T/N$
  where T is number of turning points in a time series

→ to provide a fast and simple estimate of the Hurst exponent
→ to differentiate between different types of colored noise, $P(f) \propto 1/f^{\beta}$, characterized by different values of β

Optical variability study of all blazar candidates
fitted models

- 23 sources with PL model, i.e. 10 FSRQs and 13 BL Lacs
- 15 sources with SBPL model, i.e. 13 FSRQs and 2 BL Lacs
- 6 sources with PL and SBPL models, i.e. 4 FSRQs and 2 BL Lacs

FSRQ 20

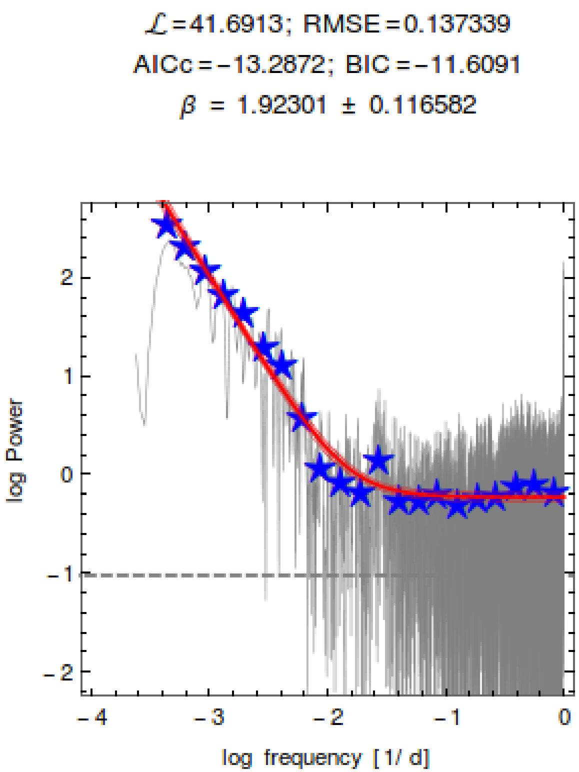

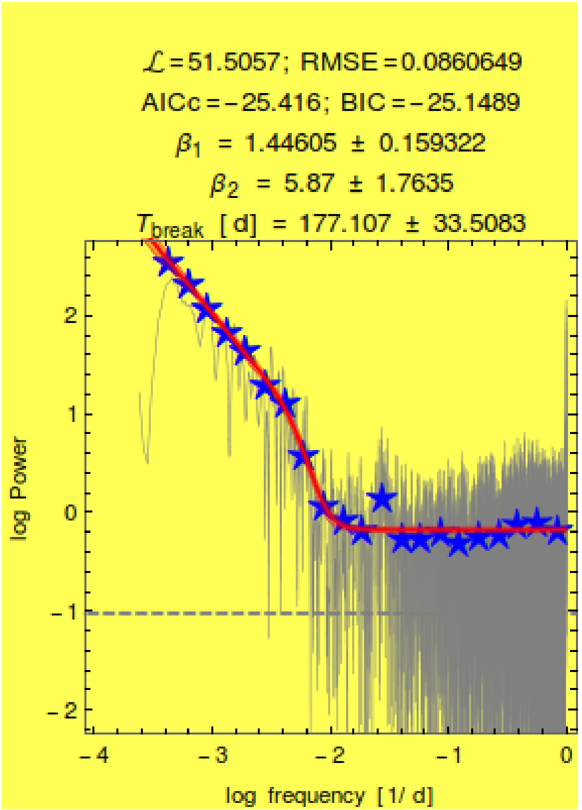

→ FSRQs' PL exponent β mostly lies in the range (1, 2)
→ one object has a flat PSD, β ≈ 0
→ BL Lacs are slightly flatter, spanning mostly the range (1, 1.8)
→ one BL Lac has a flat PSD
→ three BL Lacs have steeper PSDs, with β ∼ 3 − 4

Optical variability study of all blazar candidates

A-T plane and Hurst exponents

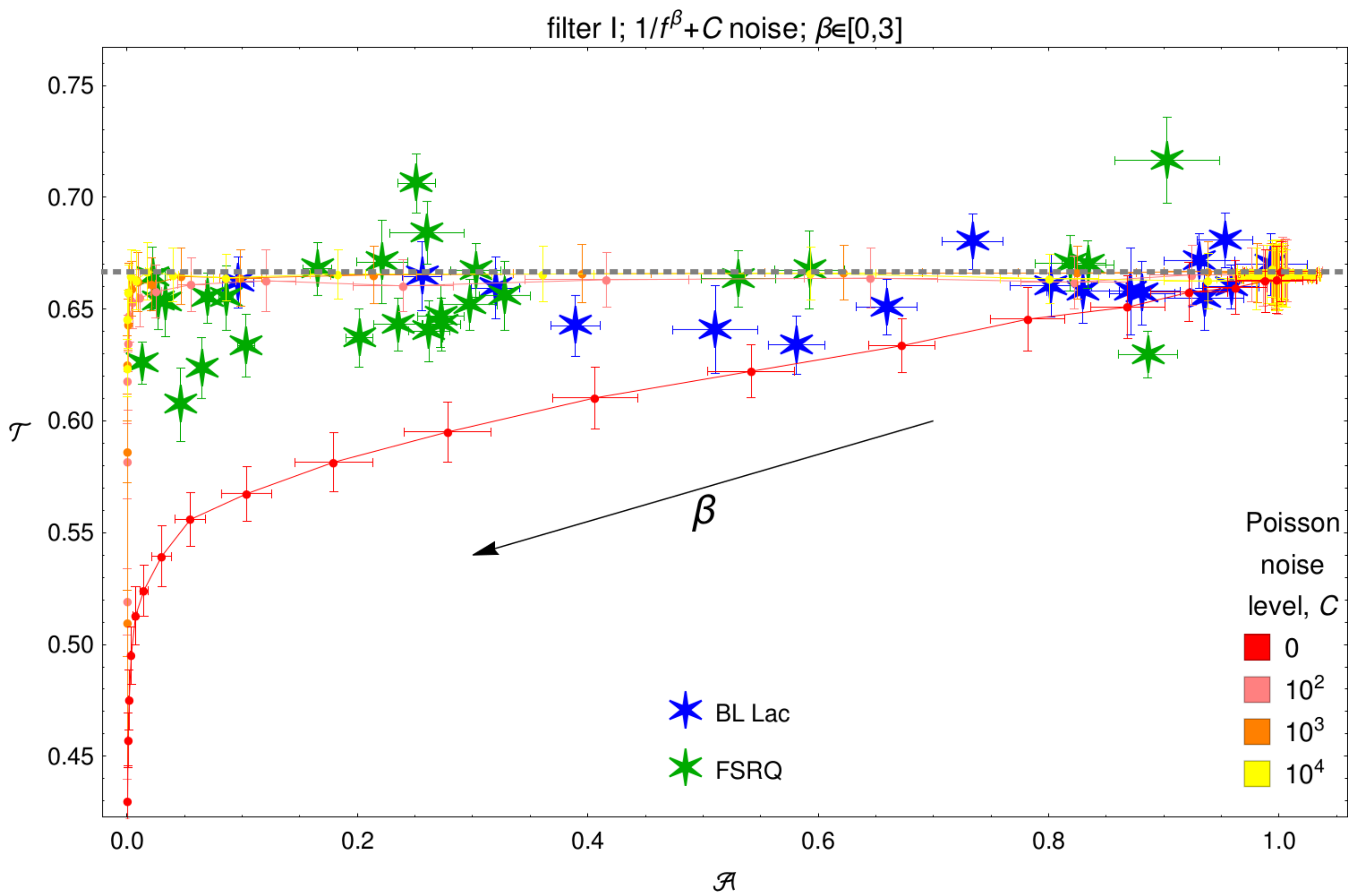

PL plus Poisson noise PSD of the form $P(f) \propto 1/f^{\beta} + C$ with $\beta \in \{0, 0.1, . . . , 3\}$

→ most objects have H ≤ 0.5 → short-term memory

→ 4 BL Lacs and 2 FSRQs have H > 0.5 → long-term memory

Optical variability study of all blazar candidates

Carma modelling

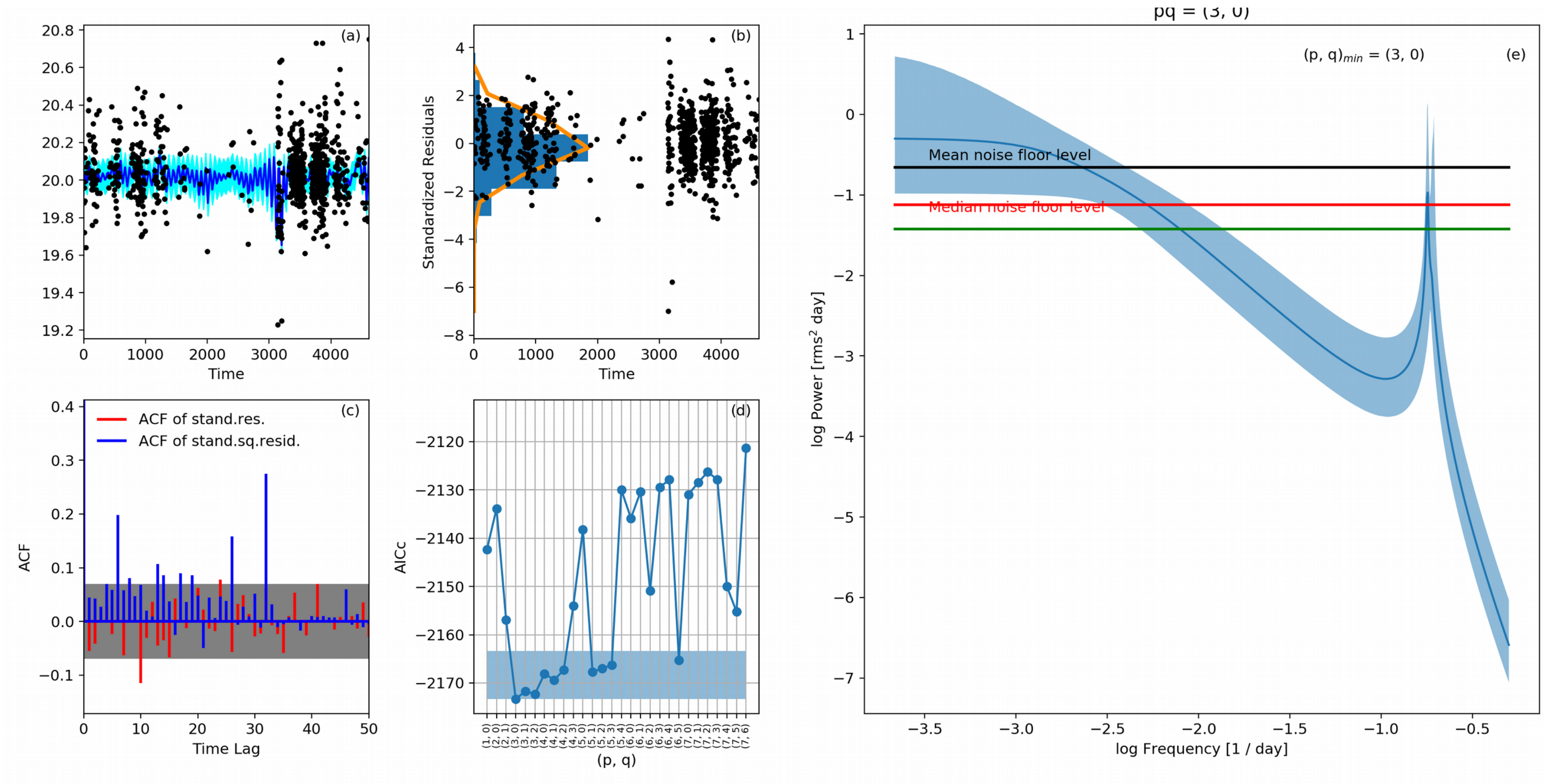

→ most of the examined objects, i.e. 18/27 FSRQs and 13/17 BL Lacs, are well described by a CARMA(2, 1) process

→ This simplest model, with a single-Lorentzian PSD, is in turn the best fit for only 3/27 FSRQs and 2/17 BL Lacs

Object	$\beta_{\rm PL}$	β_1	β_2	$T_{\rm break}$ [d]	Best model	$\log M_{\rm BH}$	H	$T_{\rm break}$ [d]	QPO [d]	CARMA order
(1)	(2)	(3)	(4)	(5)	(6)	(7)	(8)	(9)	(10)	(11)
FSRQ type blazar candidates										
J0054−7248	1.21 ± 0.13	—	—	—	PL	—	0.42 ± 0.02	—	—	(2,1)
J0114−7320⋆	1.45 ± 0.18	0.37 ± 0.40	4.53 ± 1.56	338 ± 127	SBPL	(9.32, 10.45)	0.06 ± 0.04	246	—	(2,1)
J0120−7334⋆	1.86 ± 0.15	1.28 ± 0.23	5.00 ± 1.91	229 ± 75	SBPL	(9.06, 10.14)	0.04 ± 0.03	—	—	(3,2)
J0122−7152	1.45 ± 0.17	1.01 ± 0.27	5.65 ± 4.35	155 ± 61	PL, SBPL	(8.97, 10.11)	0.24 ± 0.04	—	—	(2,1)
J0442−6818⋆	1.75 ± 0.27	0.83 ± 0.31	8.93 ± 5.20	241 ± 51	SBPL	(9.27, 10.24)	0.04 ± 0.03	363	—	(4,2)
J0445−6859	1.30 ± 0.29	—	—	—	PL	—	0.31 ± 0.05	—	—	(2,1)
J0446−6758	1.60 ± 0.18	—	—	—	PL	—	0.45 ± 0.05	—	—	(2,1)
J0455−6933	1.58 ± 0.28	0.30 ± 0.36	6.83 ± 3.38	250 ± 58	SBPL	(9.20, 10.19)	0.25 ± 0.05	—	—	(1,0)
J0459−6756	1.64 ± 0.27	0.88 ± 0.44	6.56 ± 5.47	246 ± 103	PL, SBPL	(9.01, 10.18)	0.21 ± 0.03	—	—	(3,2)
J0510−6941	1.63 ± 0.13	0.96 ± 0.16	5.75 ± 1.58	218 ± 39	SBPL	(9.22, 10.16)	0.04 ± 0.03	—	—	(2,1)
J0512−7105	0.14 ± 1.56	—	—	—	PL	—	0.63 ± 0.05	—	—	(2,1)
J0512−6732⋆	1.00 ± 0.12	0.64 ± 0.09	6.84 ± 3.26	67 ± 10	SBPL	(8.49, 9.40)	0.85 ± 0.03	—	—	(2,1)
J0515−6756	1.40 ± 0.24	—	—	—	PL	—	0.38 ± 0.02	—	—	(2,1)
J0517−6759	1.23 ± 0.21	0.70 ± 0.30	6.66 ± 6.04	164 ± 56	PL, SBPL	(9.16, 10.25)	0.29 ± 0.04	—	—	(1,0)
J0527−7036	1.26 ± 0.13	1.06 ± 0.22	3.82 ± 3.69	48 ± 34	PL	(8.18, 9.73)	0.04 ± 0.03	—	1.48	(4,3)
J0528−6836	1.47 ± 0.15	—	—	—	PL	—	0.26 ± 0.05	—	—	(2,1)
J0532−6931	1.29 ± 0.14	0.68 ± 0.21	4.33 ± 1.76	115 ± 45	SBPL	(8.76, 9.90)	0.07 ± 0.03	—	—	(3,2)
J0535−7037	1.11 ± 0.14	—	—	—	PL	—	0.42 ± 0.03	—	—	(2,1)
J0541−6800	1.56 ± 0.15	0.71 ± 0.34	3.35 ± 1.00	319 ± 172	SBPL	(9.16, 10.47)	0.08 ± 0.05	—	—	(2,1)
J0541−6815	1.92 ± 0.12	1.45 ± 0.16	5.87 ± 1.76	177 ± 34	SBPL	(9.03, 9.98)	0.21 ± 0.03	440	—	(2,1)
J0547−7207	1.37 ± 0.21	0.29 ± 0.37	4.66 ± 2.00	284 ± 106	SBPL	(9.28, 10.40)	0.03 ± 0.02	—	—	(2,1)
J0551−6916⋆	1.46 ± 0.22	0.75 ± 0.31	7.36 ± 5.21	225 ± 64	SBPL	(9.01, 10.00)	0.06 ± 0.04	—	—	(2,1)
J0551−6843⋆	1.48 ± 0.17	—	—	—	PL	—	0.11 ± 0.04	—	—	(2,1)
J0552−6850	1.62 ± 0.14	−0.70 ± 0.76	2.36 ± 0.28	1201 ± 417	SBPL	(9.74, 10.84)	0.22 ± 0.05	—	—	(2,1)
J0557−6944	1.57 ± 0.24	—	—	—	PL	—	0.49 ± 0.05	—	—	(1,0)
J0559−6920	1.44 ± 0.19	0.79 ± 0.33	5.51 ± 3.57	248 ± 93	PL, SBPL	(9.02, 10.15)	0.22 ± 0.03	—	—	(2,1)
J0602−6830	1.35 ± 0.13	0.30 ± 0.69	2.25 ± 0.68	538 ± 579	SBPL	< 10.79	0.07 ± 0.04	479	—	(4,2)
BL Lac type blazar candidates										
J0039−7356	1.61 ± 0.28	—	—	—	PL	—	0.44 ± 0.03	—	—	(2,1)
J0111−7302⋆	1.76 ± 0.44	—	—	—	PL	—	0.35 ± 0.04	—	—	(2,1)
J0123−7236	4.02 ± 1.23	—	—	—	PL	—	—	—	—	(2,1)
J0439−6832	0.98 ± 0.22	—	—	—	PL	—	0.60 ± 0.06	—	—	(2,1)
J0441−6945	1.20 ± 0.16	—	—	—	PL	—	0.45 ± 0.03	—	—	(2,1)
J0444−6729	1.47 ± 0.21	1.00 ± 0.48	4.42 ± 4.20	193 ± 133	PL	—	0.21 ± 0.05	—	—	(1,0)
J0446−6718	3.5 ± 1.13	—	—	—	PL	—	0.58 ± 0.05	—	—	(2,1)
J0453−6949	2.64 ± 0.66	—	—	—	PL	—	0.48 ± 0.04	—	—	(2,1)
J0457−6920	1.03 ± 0.18	—	—	—	PL	—	0.26 ± 0.03	—	—	(2,1)
J0501−6653⋆	1.44 ± 0.20	0.98 ± 0.32	6.95 ± 6.63	217 ± 78	PL, SBPL	—	0.29 ± 0.04	25; 89	—	(2,1)
J0516−6803	0.00 ± 0.93	—	—	—	PL	—	0.62 ± 0.05	706	5.54	(3,0)
J0518−6755⋆	1.34 ± 0.15	0.84 ± 0.33	3.75 ± 2.28	182 ± 118	PL, SBPL	—	0.18 ± 0.03	—	6.53	(3,0)
J0521−6959	1.18 ± 0.11	0.54 ± 0.26	2.94 ± 0.92	192 ± 112	SBPL	—	0.06 ± 0.04	—	—	(2,1)
J0522−7135	1.16 ± 0.39	—	—	—	PL	—	0.39 ± 0.04	—	—	(2,1)
J0538−7225	1.09 ± 0.16	0.42 ± 0.25	5.17 ± 2.86	183 ± 57	SBPL	—	0.28 ± 0.04	—	—	(2,1)

Conclusions

- The secure blazar candidates (5 FSRQs and 2 BL Lacs) have an LSP best described by the SBPL, with break time scales at 200–300 days; 1 FSRQ and 1 BL Lac are consistent with the PL PSD;

- For FSRQs such a break is not really surprising, i.e. they can be interpreted as disk dominated. But the two BL Lacs with a broken PSD are interesting, as BL Lacs are believed to be jet dominated;

- the steepness of the high frequency component of the SBPL is intriguing: it can indicate a new class of AGNs, or it can be a sign of a double BH system, where the shorter time scale variability from the disk is wiped out - the accretion disk surrounds both BHs, outside their orbit.

Further directions

Look for high and very high energy coincidences:

- Chandra
- Fermi-LAT
- H.E.S.S.